

A New Similarity Measure for Nonrigid Volume Registration Using Known Joint Distribution of Target Tissue: Application to Dynamic CT Data of the Liver

Jun Masumoto¹, Yoshinobu Sato¹, Masatoshi Hori², Takamichi Murakami²,
Takeshi Johkoh², Hironobu Nakamura², and Shinichi Tamura¹

¹ Division of Interdisciplinary Image Analysis

² Department of Radiology, Osaka University Graduate School of Medicine
Suita, Osaka, 565-0871, Japan

Abstract. A new similarity measure for volume registration is proposed, which uses using the assumption that the joint distribution of a target tissue is known. This similarity measure is designed so that it can deal with the tissue slide that occurs at boundaries between the target tissue and other tissues. Pre-segmentation of the target tissue is unnecessary. We intend to apply the proposed measure to registering volumes acquired at different time-phases in dynamic CT scans of the liver using contrast materials. In order to derive the similarity measure, we first formulate the ideal case where the joint distributions of all the tissues are known, after which we derive the measure for a realistic case where only the joint distribution of the target tissue is known. We applied the proposed measure experimentally to eight dynamic CT data sets of the liver. After describing a practical method for estimating the joint distribution of the liver from real CT data, we show that the problem of tissue slide is effectively dealt with using the proposed measure.

1 Introduction

Dynamic contrast-enhanced CT scans are effective means of disease diagnosis and surgical planning for the liver. In a dynamic CT study, several CT volumes are typically acquired at different time-phases not in a single breath-hold. Hence, these volumes are not guaranteed to be registered between different time-phases due to respiratory motion. Their registration by post-processing is highly desirable on account of the following advantages: (1) Accurate correlation between different time-phase images can be performed. (2) In 3D rendering of the liver, portal/hepatic veins and tumors, which are enhanced at different phases, can be registered more accurately. (3) Time-density curves can be estimated at every voxel, which should eventually permit automatic cancer characterization [1].

In this paper, we address the problem of nonrigid registration between volumes acquired at different time-phases of dynamic CT scans of the liver. An important issue in registration of the liver is tissue slide, which occurs along

boundaries between the liver and other tissues, resulting in discontinuities in the 3D vector field describing the nonrigid deformation [2] [3]. Previous attempts to deal with this problem have required pre-segmentation of the liver region [4] or specification of places where tissue slide may occur before registration [5]. However, because segmentation of the liver from CT data is a far from easy task [6], the ability to employ direct registration between raw CT volumes without segmentation is desirable in the clinical environment.

As a means of dealing with tissue slide without pre-segmentation, we propose a new similarity measure for volume registration. In the dynamic CT, the tissue contrast during scans at different time-phases changes differently depending on the particular tissue involved. Thus, unlike a cross-correlation measure, a new similarity measure should also be able to cope with differences in contrast between volumes to be registered. Although mutual information [7] (or the entropy correlation coefficient: ECC [8]) is known to be useful as a similarity measure in such a case [9] [10], we instead employ the following assumption: “The joint distribution of a target tissue is known.” The use of the known joint distribution was originally suggested by Leventon *et al.* [11]. The main difference between their method and ours is that we utilize the known joint distribution of only the target tissue while they use that of the entire volume. Thus, our method tries to register only the target tissue, for example, the liver, but ignores non-target tissues. By taking this approach, we effectively cope with tissue slide which is inevitable in registration of the abdominal domain.

2 Theory

2.1 Ideal Case: Assuming Joint Distributions of All Tissues Are Known

We consider the joint distribution $P_o(I, J)$ of two volumes whose intensity values are represented by I and J , respectively. These two volumes are assumed to be correctly registered. If we assume that the volume consists of the tissue set $\Gamma = \{\gamma_1, \gamma_2, \dots, \gamma_n\}$ and the joint conditional distribution for each tissue is known, $P_o(I, J)$ can be decomposed into

$$P_o(I, J) = \sum_{\gamma \in \Gamma} P(I, J, \gamma) = \sum_{\gamma \in \Gamma} P(I, J|\gamma) \cdot P(\gamma), \quad (1)$$

where $\sum_{\gamma \in \Gamma} P(\gamma) = 1$. In this case, an optimal similarity measure, $B(X)$, should be maximum when $X = P_o(I, J)$ is satisfied. Here, we introduce a concept that we call “exclusive”. We define $P(I, J|\gamma_i)$ as being “exclusive” if $P(I, J|\gamma_i)$ satisfies the following conditions for all γ_i ($1 \leq i \leq n$):

$$\begin{aligned} & \forall (I_0, J_0) \{ (I_0, J_0) | P(I_0, J_0|\gamma_i) \neq 0 \}, \\ & \sum_{\substack{\gamma_k \in \Gamma \\ k \neq i}} \sum_J P(I_0, J|\gamma_k) = 0 \quad \wedge \quad \sum_{\substack{\gamma_k \in \Gamma \\ k \neq i}} \sum_I P(I, J_0|\gamma_k) = 0. \end{aligned} \quad (2)$$

Using the “exclusive” condition, $B(X)$ can be decomposed into

$$\begin{aligned}
 B(X) &= \sum_{\gamma \in \Gamma} W_{\gamma} \cdot T_{\gamma}(X) \\
 &= W_{\gamma_1} \cdot T_{\gamma_1}(X) + W_{\gamma_2} \cdot T_{\gamma_2}(X) + \cdots + W_{\gamma_n} \cdot T_{\gamma_n}(X), \quad (3)
 \end{aligned}$$

where $T_{\gamma_i}(X)$ is maximum when γ_i is correctly registered (that is, when $X = P(I, J|\gamma_i)$), and W_{γ_i} is its weight coefficient satisfying $\sum_{\gamma \in \Gamma} W_{\gamma} = 1$. By substituting P_o for X in $B(X)$, we have

$$\begin{aligned}
 B(P_o) &= \sum_{\gamma \in \Gamma} W_{\gamma} \cdot T_{\gamma}(P_o) \\
 &= W_{\gamma_1} \cdot T_{\gamma_1}(P_o) + \cdots + W_{\gamma_i} \cdot T_{\gamma_i}(P_o) + \cdots + W_{\gamma_n} \cdot T_{\gamma_n}(P_o). \quad (4)
 \end{aligned}$$

Using the exclusive condition, $T_{\gamma_i}(P_o)$ is described as

$$\begin{aligned}
 T_{\gamma_i}(P_o) &= T_{\gamma_i}(P(I, J|\gamma_1) \cdot P(\gamma_1)) + T_{\gamma_i}(P(I, J|\gamma_2) \cdot P(\gamma_2)) \\
 &\quad + \cdots + T_{\gamma_i}(P(I, J|\gamma_i) \cdot P(\gamma_i)) + \cdots + T_{\gamma_i}(P(I, J|\gamma_n) \cdot P(\gamma_n)) \\
 &= 0 + 0 + \cdots + P(\gamma_i) \cdot T_{\gamma_i}(P(I, J|\gamma_i)) + \cdots + 0 \\
 &= P(\gamma_i) \cdot T_{\gamma_i}(P(I, J|\gamma_i)). \quad (5)
 \end{aligned}$$

Therefore, $T_{\gamma_i}(X)$ should be maximum when $X = P(I, J|\gamma_i)$.

2.2 Realistic Case: Assuming Joint Distribution of One Target Tissue Is Known

Here, we consider a more realistic case. We assume that our target for registration is only liver tissue. Let the tissue set Γ consist of only two tissues, liver (L) and others (O), where O represents all the tissues except liver. When the occurrence probability of liver is $P(L) = \alpha$, that of the others is $P(O) = 1 - \alpha$. Using Equation (1), we therefore have

$$P_r(I, J) = \alpha \cdot P(I, J|L) + (1 - \alpha) \cdot P(I, J|O). \quad (6)$$

As a practical supposition, we assume that the joint conditional distribution of liver tissue, $P(I, J|L)$, is known, while $P(I, J|O)$ is unknown. By assuming that $P(I, J|L)$ and $P(I, J|O)$ are exclusive, we have

$$B(X) = W_L \cdot T_L(X) + W_O \cdot T_O(X). \quad (7)$$

By substituting P_r for X ,

$$\begin{aligned}
 B(P_r) &= W_L \cdot T_L(P_r) + W_O \cdot T_O(P_r) \\
 &= \alpha \cdot W_L \cdot T_L(P(I, J|L)) + (1 - \alpha) \cdot W_L \cdot T_L(P(I, J|O)) \\
 &\quad + \alpha \cdot W_O \cdot T_O(P(I, J|L)) + (1 - \alpha) \cdot W_O \cdot T_O(P(I, J|O)). \quad (8)
 \end{aligned}$$

Since $P(I, J|L)$ and $P(I, J|O)$ are exclusive, $T_L(X)$ and $T_O(X)$ should satisfy the following conditions:

- ||1|| $T_L(X)$ is zero when $X = P(I, J|O)$.
- ||2|| $T_O(X)$ is zero when $X = P(I, J|L)$.
- ||3|| $T_L(X)$ is maximum when $X = P(I, J|L)$.
- ||4|| $T_O(X)$ is maximum when $X = P(I, J|O)$.

It should be noted here that $P(I, J|O)$ is unknown. Thus, the above condition ||4|| should be satisfied for any possible $P(I, J|O)$. Our aim is to derive a similarity measure satisfying the above four conditions.

2.3 Derivation of Similarity Measure for the Realistic Case

We assume that $P(I, J|L)$ is well-approximated by the gaussian function given by

$$P(I, J|L) = \frac{1}{\sqrt{2\pi}|\Sigma|} e^{-\frac{1}{2}((I, J) - (\bar{I}, \bar{J}))^T \Sigma^{-1} ((I, J) - (\bar{I}, \bar{J}))}, \quad (9)$$

where (\bar{I}, \bar{J}) and Σ are the average values and covariance matrix, respectively.

In order to obtain an approximated similarity measure satisfying the above four conditions, we use

$$\begin{aligned} T_L(X) &= \sum_{I, J} \{F_L(I, J) \cdot X(I, J)\} \\ T_O(X) &= \sum_{I, J} \{F_O(I, J) \cdot X(I, J)\}, \end{aligned} \quad (10)$$

where

$$F_L(I, J) = e^{-\frac{1}{2}((I, J) - (\bar{I}, \bar{J}))^T \Sigma^{-1} ((I, J) - (\bar{I}, \bar{J}))} \quad (11)$$

$$F_O(I, J) = 1 - \max \left\{ e^{-\frac{(I - \bar{I}')^2}{2\sigma_{I'}^2}}, e^{-\frac{(J - \bar{J}')^2}{2\sigma_{J'}^2}} \right\}, \quad (12)$$

in which \bar{I}' and \bar{J}' are average values of the projections of $P(I, J|L)$ onto the I -axis and J -axis, and $\sigma_{I'}$ and $\sigma_{J'}$ are their variances. Finally, we have the similarity measure $B(X)$ given by

$$B(X) = \beta \cdot T_L(X) + (1 - \beta) \cdot T_O(X). \quad (13)$$

3 Experiments

3.1 Method for Estimating Joint Distribution of the Liver

We have assumed that the joint distribution of a target tissue is known. To apply the theory described in the previous section, a practical method of estimating the

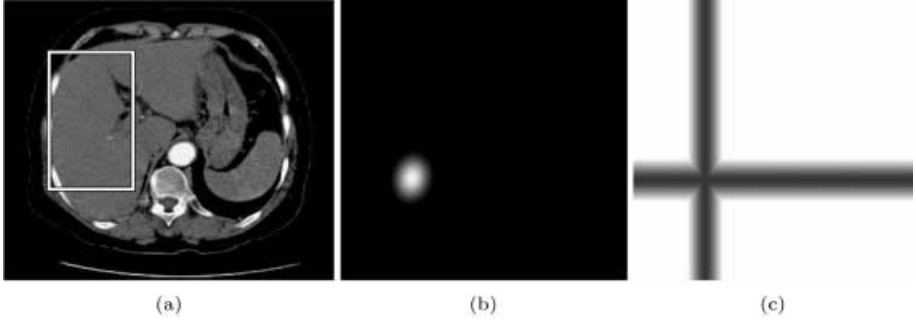


Fig. 1. Method for estimating joint distribution of the liver. (a) Volume of interest (VOI) used for the estimation. (b) Estimated $F_L(I, J)$ (Equation (11)). (c) Estimated $F_O(I, J)$ (Equation (12)).

joint distribution of a target tissue from two unregistered volumes is necessary. The field of view (FOV) for abdominal CT scans is usually set based on the spine position. We set the volume of interest (VOI) so that it would be mostly occupied by liver tissue (Fig. 1(a)). The position of the VOI could be fixed for each patient since the position of the liver relative to the spine was not greatly different in each case. We estimated the averages (\bar{I}, \bar{J}) and covariance matrix Σ of the joint probability distribution $P(I, J|L)$ of Equation (9) by analyzing the joint histogram inside the VOI of the two volumes. (\bar{I}, \bar{J}) and Σ were estimated from the histogram region whose center was the mode of the joint histogram and whose horizontal and vertical widths were three times the full width half maximum (FWHM) values of 1D histograms projected onto the I - and J -axes, respectively. Although the two volumes were not registered at this point, it still gave a good approximation. Figure 1 shows an example of the above estimation.

3.2 Registration Method

Nonrigid volume registration methods are typically comprised of three steps: definition of the similarity measure, representation of the deformation, and maximization of the defined similarity measure. With respect to the latter two steps, we employed an existing nonrigid registration method using free-form deformation by a hierarchical B-spline grid proposed by Rueckert *et al.* [2]. The hierarchical grid consisted of three levels: 42 mm, 21 mm, and 10.5 mm. We embedded the proposed similarity measure and the entropy correlation coefficient (ECC), which is essentially equivalent to normalized mutual information [8], into the registration method, and compared these two different similarity measures. The parameter value employed in Equation (13) was $\beta = 0.5$.

3.3 CT Data Sets

Eight data sets of dynamic CT scans of the liver acquired at Osaka University Hospital and the National Cancer Center were used for performance evaluation.

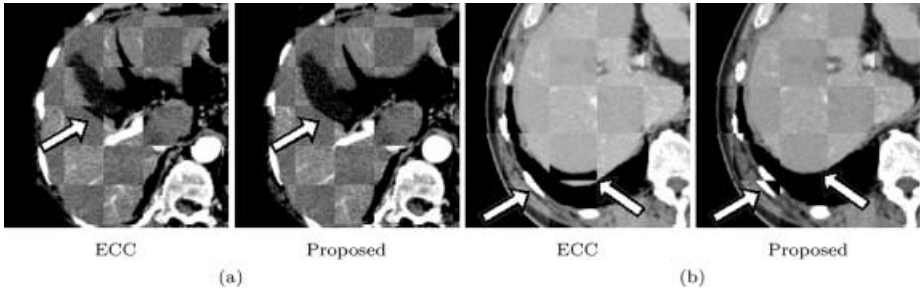


Fig. 2. Illustrative examples of registration results. (a) Left: ECC (which is equivalent to normalized mutual information). Right: Proposed similarity measure. (b) Left: ECC. Right: Proposed similarity measure.

Table 1. Summary of evaluation results. The quality of the registration results is ranked into five groups based on the visually observed discrepancy: A (discrepancy 0 – 2 mm), B (2–4 mm), C (4–6 mm), D (6–8 mm), E (8– mm).

Case #	Imaging conditions				Evaluation		
	Thickness (Interval)	FOV	Phase 1	Phase 2	Initial	Proposed	ECC
1	2.5 mm (1.25 mm)	34 × 34 cm ²	early arterial	portal	E	A	C
2	2.5 mm (1.25 mm)	34 × 34 cm ²	early arterial	portal	C	A	B
3	2.5 mm (1.25 mm)	34 × 34 cm ²	early arterial	portal	E	A	C
4	2.5 mm (1.25 mm)	34 × 34 cm ²	early arterial	portal	C	A	A
5	2.0 mm (1.0 mm)	28 × 28 cm ²	pre-contrast	portal	D	A	C
6	2.0 mm (1.0 mm)	32 × 32 cm ²	pre-contrast	portal	C	A	B
7	2.0 mm (1.0 mm)	32 × 32 cm ²	pre-contrast	portal	B	A	A
8	2.0 mm (1.0 mm)	32 × 32 cm ²	pre-contrast	portal	E	E	E

The imaging conditions are summarized in Table 1. Each CT data set originally consisted of volumes at three or four different time-phases, out of which two phases were registered. One was before the injection of the contrast material (pre-contrast) or the early arterial phase (when the effect of the contrast material is small); the other was the portal phase (when the effect of contrast enhancement is large). Because the volumes at these two phases were not acquired in a single breath-hold, there was a possibility of deformation between them due to respiratory motion. The original volume size was 512 × 512 × 150–200 (voxels), which was reduced to half size along each axis direction.

3.4 Results

Table 1 summarizes the evaluation results for the eight data sets. In the evaluation, we classified the quality of the registration results into five groups (see caption of Table 1) based on visually observed discrepancy throughout the volumes. Registration error was reduced from the initial states in the both proposed and ECC measures, but the proposed similarity measure was more effective. Fig-

ure 2 shows illustrative examples of comparisons between the proposed measure and ECC. Two volumes are displayed using the checker-board method. In Fig. 2(a), tissue slide between the liver and the gallbladder is evident. Using the proposed method, the boundaries of the liver are continuous in the checker-board display, which means they are well-registered, whereas the boundaries are not well-registered in the two volumes using ECC. In Fig. 2(b), the ribs are well-registered but the liver is not using ECC. In this case, even though the ribs and liver are in close proximity, their motions were largely dissimilar and there is discontinuity in the deformation field between them. The liver is well-registered using the proposed measure since it tracked only liver tissue. However, it should be noted that the boundary of the ribs is not well-registered since the joint distribution of the ribs (bone tissue) differs from the known distribution.

4 Discussion

For application to dynamic CT data of the liver, the proposed measure showed better results than ECC. The reason is considered to be that the new method can more effectively deal with tissue slide. Using the proposed measure, the registration process does not try to register the entire volume but only those regions having the known joint distribution. It simply ignores non-target tissues. Consequently, it is not affected by discontinuities in the deformation field that occur at boundaries of two tissues. In fact, the rib boundary (Fig. 2(b)) was not well-registered using the proposed method, but this is not considered disadvantageous because the aim is to register only the target (i.e. liver) tissue.

The proposed similarity measure assumes that the joint distribution of the target tissue is known. One problem is how this should be estimated. The method using histogram analysis of the fixed VOI, explained above in section 3.1, was quite effective so long as the relative position of the target tissue in the FOV was roughly determined. We applied the method to CT data sets acquired at two hospitals and confirmed that the liver region inside the VOI was more than 50% of the entire VOI. The estimation was successful with all the data sets used in our experiments.

It should be noted that the boundaries of the target tissue are appropriately registered based on the proposed similarity measure, though the information provided on intensity patterns may be insufficient for registering the inner part of the tissue. The deformation field is considered to be estimated mostly based on B-spline interpolation in the inner part. One approach to addressing this problem would be to use a biomechanically appropriate interpolation method rather than B-splines.

5 Conclusion

We have proposed a novel similarity measure for volume registration when the joint distribution of a target tissue is known. Application of the proposed measure to dynamic CT data sets of the liver confirmed that it could effectively deal with

tissue slide without the need for any pre-segmentation or manual interaction. We further showed a method for estimating a good approximation of the joint distribution of the target tissue from two unregistered volumes. The proposed measure works well for registering the boundaries of the target tissue, while the registration of the inner part of the tissue is estimated mostly based on B-spline interpolation. Future problems include quantitative evaluation of the proposed similarity measure and developing a post-processing method able to register the inner part of a tissue by taking intensity patterns into account.

Acknowledgements

This work was partly supported by JSPS Research for the Future Program JSPS-RFTF99I00903 and JSPS Grant-in-Aid for Scientific Research (B)(2) 12558033.

References

1. Andress Carrillo, Jeffrey L. Duerk, Jonathan S. Lewin, and David L. Wilson. Semi-automatic 3-D Image Registration as Applied to Interventional MRI Liver Cancer Treatment. *IEEE Trans. Med. Imaging*, 19(3):175-185, 2000.
2. D.Rueckert, L.I.Sonoda, C.Hayes, D.L.G.Hill, M.O.Leach, D.J.Hawkes. Nonrigid Registration Using Free-Form Deformations: Application to Breast MR Images. *IEEE Trans. Med. Imaging*, 18(8):712-721, 1999.
3. H. Lester and S.R. Aridge. A survey of hierarchical non-linear medical image registration. *Pattern Recognition*, 32:71-86, 1999.
4. Mi Chen, Takeo Kanade, Dean Pomerleau, Jeff Schneider. 3D Deformable Registration of Medical Images Using a Statistical Atlas. *Lecture Notes in Computer Science*, 1679 (*MICCAI'99*): 621-630, 1999.
5. Yongmei Wang, Lawrence H Staib. Physical model-based non-rigid registration incorporation statistical shape information. *Medical Image Analysis*, 4:7-20, 2000.
6. Andrea Schenk, Guido Prause, and Heinz-Otto Peitgen. Efficient Semiautomatic Segmentation of 3D Objects in Medical Images. *Lecture Notes in Computer Science*, 1935 (*MICCAI2000*): 186-195, 2000.
7. William M. Wells III, Paul Viola, Hideki Atsumi, Shin Nakajima and Ron Kikinis. Multi Modal volume registration by maximization of mutual information. *Medical Image Analysis*, 1(1):35-51, 1996.
8. Josien P.W. Pluim, J.B. Antoine Maintz, and Max A. Viergever. Interpolation Artifacts in Mutual Information-Based Image Registration. *Computer Vision and Image Understanding*, 77:211-232, 2000.
9. Mark Holden, Derek L. G. Hill, Erika R. E. Denton, Jo M. Jarosz, Tim C. S. Cox, Trosten Rohlfing, Joanne Goodey, David J. Hawkes. Voxel Similarity Measures for 3-D Serial MR Brain Image Registration. *IEEE Trans. Med. Imaging*, 19(2):94-102, 2000.
10. Alexis Roche, Gregoire Malandain, Nicholas Ayache, and Sylvain Prima. Toward a Better Comprehension of Similarity Measures Used in Medical Image Registration. *Lecture Notes in Computer Science*, 1679 (*MICCAI'99*): 555-566, 1999.
11. Michael E. Leventon and W. Eric L. Grimson. Multi-Modal Volume Registration Using Joint Intensity distributions. *Lecture Notes in Computer Science*, 1496 (*MICCAI'98*): 1057-1066, 1998.